





# A Probability-Based Optimization Approach for Entanglement Distribution and Source Position in Quantum Networks

Giovanni Iacovelli , *Member, IEEE*, Francesco Vista , *Graduate Student Member, IEEE*, Nicola Cordeschi , *Member, IEEE*, and Luigi Alfredo Grieco , *Senior Member, IEEE*

**Abstract**—Quantum Internet (QI) is a system of interconnected quantum computers able to exchange information encoded in the so called quantum bits (qubits). Differently from the classical counterpart, qubits benefit from a manifold properties guaranteed by quantum mechanics, such as superposition and entanglement. Despite the fact that quantum networks bring significant advantages, several phenomena can negatively impact the overall system, potentially hindering communication. In order to evaluate the network performance, a comprehensive probability expression is derived in this work to ultimately determine how many qubits are expected to be successfully received by nodes. On this basis, a Mixed-Integer Non-Linear Programming (MINLP) problem is formulated to fairly maximize the qubits exchanged between node pairs and jointly optimize (i) the position of the quantum source, and (ii) the entanglement distribution plan. To cope with the non-convexity of the problem, an iterative optimization algorithm, leveraging Block Coordinate Descent (BCD) and Successive Convex Approximation (SCA) techniques, is proposed. A thorough simulation campaign is conducted to corroborate the theoretical findings. Numerical results demonstrates, under different parameter setups, that the proposed algorithm provides superior performance with respect to a baseline approach.

**Index Terms**—Quantum Networks, Probabilistic Modeling, Optimization, Teleportation Protocol.

## I. INTRODUCTION

Quantum computing [1] is widely considered an emerging paradigm that holds the potential to solve specific challenging problems more efficiently than classical computers [2]. The basic unit of quantum information is the quantum bit (qubit), which is a two-level quantum system, representing the foundation of quantum devices and hence of quantum computing. Qubits can be physically represented as single atoms, photons or a cold superconducting circuits with moving electrons [3]. Unlike classical bits, a qubit has the unique ability to

simultaneously exist in two states until a measurement is performed. This property, namely superposition, is granted by quantum mechanics and allows quantum computers to exponentially increase their computational power with the number of qubits [4].

Despite the significant advantages introduced by qubits, they are highly susceptible to environmental noise, which can lead to decoherence, resulting in an undesired transition to classical states. In addition, quantum gates [5] applied to qubits may introduce further errors and are restricted by coherence time. Thus, to effectively harness the benefits of quantum computing, a large number of high-quality qubits with long decoherence times is required [6]. However, current devices lack the necessary capabilities to control a significant number of qubits and hence to effectively perform practical tasks.

To address these and other important issues, Quantum Internet (QI) has been introduced [7]–[9] as a cutting-edge technology and communication paradigm. Among the vast plethora of possible applications, quantum networks can be employed to overcome the current computational power limitations. For instance, the scientific community envisions the integration of quantum computing devices at the edge of 6G networks as a mean to enhance service provisioning [10]. Indeed, thanks to QI, in the near future multiple qubit-limited devices will be interconnected to share quantum states among each other [11] through a quantum channel, i.e., fiber or free space optical links. However, even if the state of a qubit can be directly encoded by using the polarization of a photon, it may be lost due to attenuation or noise. In such cases, the quantum information is irretrievably destroyed, and it cannot be recovered through measurement or copying, as stated by the postulate of quantum measurement and the no-cloning theorem. Thus, a common employed approach is to generate and distribute a particular two-qubit state to remote nodes, leveraging the entanglement phenomenon [12]. Indeed, when two particles are entangled, the quantum state of one particle becomes correlated with the state of the other, regardless of the distance between them. This unique property, along with the transmission of classical information, is at the basis of the quantum teleportation protocol [13]. Nevertheless, due to attenuation in the medium, the entanglement distribution exponentially decreases over distance. Additionally, the presence of noise during the generation process or entanglement decoherence can produce an imperfect entangled state or cause the transition to an undesired one, making it unusable for a

This work was partially supported by the European Union under the Italian National Recovery and Resilience Plan (NRRP) of NextGenerationEU, with particular reference to the partnership on “Telecommunications of the Future” (PE00000001 - program “RESTART”, CUP: D93C22000910001) and to the national center on “Sustainable Mobility” (CN00000023 - program “MOST”, CUP: D93C22000410001). It was also supported by the PRIN project no. 2017NS9FEY entitled “Realtime Control of 5G Wireless Networks: Taming the Complexity of Future Transmission and Computation Challenges” funded by the Italian MUR, by “The house of emerging technologies of Matera (CTEMT)” project funded by the Italian MIMIT, and by the PON AGREED projects (ARS01 00254) funded by the Italian MUR.

G. Iacovelli, F. Vista, N. Cordeschi, and L.A. Grieco are with the Department of Electrical and Information Engineering, Politecnico di Bari, 70126 Bari, Italy (email: *name.surname@poliba.it*) and with the Consorzio Nazionale Interuniversitario per le Telecomunicazioni, 43124 Parma, Italy.

reliable teleportation operation [14].

For these reasons, the scientific community has investigated the maximization of the entanglement distribution while considering different aspects. One of them is the adoption of purification techniques [15]–[19], which enhance the goodness of an entangled state and hence of the communication as a whole. Another important considered facet is quantum memory [20]–[24], which represents one of the most constrained resources and plays a crucial role in preserving and retrieving on-demand entangled states to improve the robustness and reliability of entanglement distribution. However, these works assume that a dedicated quantum source is placed in the middle between each node. In practice, this assumption overlooks the fact that such hardware is expensive and often limited, thus potentially constraining the number of nodes in the network [25]. Moreover, the rate at which entangled particles can be generated also impacts the number of entanglement links that can be established.

To the best of the authors' knowledge, the existing scientific literature has not investigated the optimization of the quantum source position by taking into account the non-negligible failure probability associated with the photon transmission and teleport operations. These facets are of pivotal importance to ultimately improve the efficiency of the whole communication system. In this regard, this work provides several significant contributions, which are outlined below.

- A comprehensive probability expression is derived to determine how many qubits are expected to successfully arrive at the receiver. The proposed model takes into account the attenuation of the fiber, as well as the depolarizing and dephasing noise introduced during the execution of the operations related to the teleportation protocol.
- Based on the above derivation, a Mixed-Integer Non-Linear Programming (MINLP) problem is formulated to fairly maximize the number of qubits exchanged among the nodes and jointly optimize (i) the position of the quantum source, assuming to have a priori knowledge of the quantum node location, and (ii) the scheduling plan, describing how many entangled pairs should be allocated at each node couple.
- To cope with the non-convexity of the original formulation, a dedicated optimization strategy is designed. First, the Block Coordinate Descent (BCD) technique is employed to split the problem into two sub-problems. The first is initially relaxed and then exactly solved leveraging the Karush-Kuhn-Tucker (KKT) conditions [26]. Capitalizing on the first solution, the second one is addressed by adopting the Successive Convex Approximation (SCA) method.
- A simulation campaign is carried out to assess the effectiveness of this work. In particular, the derived probability expression and the proposed optimization algorithm are evaluated under different parameters, such as node topology, depolarizing and dephasing rate, fiber attenuation, and generation chance. Moreover, the algorithm is compared with a baseline approach which adopts the centroid of the nodes as the source location, while exploiting the already derived optimal scheduling plan.

The theoretical findings indicate that in case of quantum networks deployed in relatively small areas, i.e., a few square kilometers, the proposal and the baseline approach have similar performance. However, when wider areas are considered, the derived optimal solution provides a significant advantage in terms of number of qubits successfully received by the nodes. This demonstrates that the proposed algorithm is able to capture the non-linearity of the derived probability and can be employed as tool for optimal design and assessment of large-scale quantum networks.

The remainder of this work is organized as follows. Section II discusses the related works. Section III provides an introduction to quantum entanglement and teleportation protocol. Section IV describes the system model and derives the overall communication probability. Starting from the model, Section V presents the problem formulation. Hence, Section VI proposes an optimization algorithm to solve the problem. Section VII corroborates the theoretical findings and compares the obtained results against a baseline approach, under different parameter setups. Finally, Section VIII concludes the work and draws future research perspectives.

*Notation:* Boldface lower case letters refer to vectors;  $\mathbf{x}^T$  is the transpose of a generic vector  $\mathbf{x}$ ;  $|\mathbf{x}\rangle$  is the column vector of a generic quantum state  $\mathbf{x}$ ;  $\mathcal{O}(x)$  denotes the time-complexity of an algorithm of input size  $x$ , i.e, big O notation;  $\mathcal{U}(\cdot, \cdot)$ ,  $\text{Beta}(\cdot, \cdot)$ , and  $\mathcal{T}(\cdot, \cdot, \cdot)$  define the uniform, beta, and triangular distributions. The main adopted symbols of this paper are summarized in Table I.

## II. RELATED WORKS

In the literature there is a growing interest regarding several aspects of quantum communications, with the goal of maximizing the entanglement photon distribution, and hence the throughput, by considering factors such as fidelity and quantum memory.

In particular, fidelity represents the probability that a pair of entangled qubits are in the desired state, i.e., maximally entangled, which in turn affects the communication efficiency. In this context, authors in [15] investigate entanglement link fidelity by shortening the amount of time links are maintained, before swapping operations are performed. In [16], to maximize the rates in a quantum network while ensuring a minimum end-to-end fidelity requirement, the entanglement distribution problem is presented as a linear programming problem. An upper bound on the path's length is imposed to fulfill the fidelity, which lowers with each entanglement swapping operation along the path. Purification methods can be considered in cases where an entanglement link is characterized by low fidelity. Specifically, purification techniques consist in entangling multiple pairs of qubits with low fidelity and then merging them into a single one with high fidelity [27]. In this regard, [17] proposes an adaptive routing scheme to manage multiple communication requests. The approach involves a preliminary step of purifying the links, so that only the links whose fidelity is above a given threshold are used in the routing process. Similarly, authors in [18] design an algorithm to select a path which satisfies a end-to-end fidelity constraint.

[19] presents an algorithm to maximize network throughput by preparing multiple candidate entanglement paths and determining optimal purification schemes. Then, the final set of entanglement paths that maximize network throughput under the given quantum resource constraints are selected.

The other major aspect considered in the literature is quantum memory, which can store the quantum state of a photon to be used when needed. Quantum memory is a key component of quantum routers, also known as quantum repeaters, that are essential for the distribution of entangled states over long distances in large-scale quantum networks. However, the performance of quantum repeaters is far from ideal, owing to the limited quantum memory in quantum repeaters, which impairs the rate and efficiency of entanglement distribution. To overcome this challenge, in [20] it is proposed a quantum queuing model, based on dynamic programming, in order to track the delay. In particular, a policy is developed to exponentially reduce the average queuing delay with respect to memory size. The same authors, in [21], present a first entanglement distribution protocol that can achieve a high distribution rate by considering imperfect entanglement swapping operations at quantum repeaters. However, it is assumed that the quantum repeater node has unbounded memory, and the stored qubit are not affected by the decoherence phenomena, resulting in ideal fidelity. In [22], an entanglement rate optimization problem is investigated considering a system able to process a set of requests at the same time. In particular, the quantum routing problem is decoupled in i) scheduling, in which an end-to-end entanglement path is assigned to a pair of quantum nodes, and ii) path selection, where the best path is found. A novel approach for maximizing entanglement distribution rate while considering quantum repeaters with a limited memory is proposed in [23], which is subsequently decomposed into entanglement generation and swapping sub-problems. A greedy algorithm for short-distance entanglement generation is proposed, such that the quantum memories can be employed in an efficient manner. The swapping sub-problem, modeled through an entanglement graph, is solved with a heuristic technique which divides the original problem into several sub-problems, each of which can be solved in polynomial time using dynamic programming. Instead, [24] introduces a framework for optimizing the entanglement generation and distribution among quantum users having different resources and application requirements. This approach aims to optimally distribute entangled pairs among quantum users while satisfying a minimum entanglement rate requirement for each user.

Although interesting, these works consider the quantum source placed in a fixed position, e.g., the middle point among quantum nodes. Moreover, most of them, neglect the limited rate at which Bell pairs can be generated. Further, no investigations have taken into account the failure probability associated with photon transmission and teleport operations.

### III. QUANTUM ENTANGLEMENT AND TELEPORTATION

Entanglement is a fundamental property of quantum mechanics in which a pair of particles are generated in such a manner that they share a quantum state, even if they are

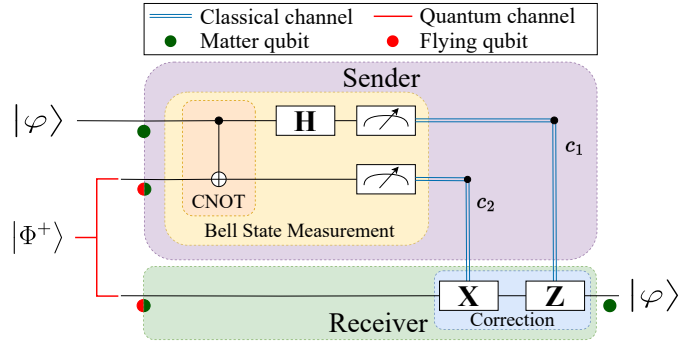


Fig. 1: Quantum teleportation circuit.

spatially separated. In this case, any quantum measurement performed on one entangled particle irreversibly affects the entire entangled state. When maximally entangled, two quantum states, also known as *Bell states* or *EPR pairs*, can be expressed [5] as:

$$|\Phi^\pm\rangle = \frac{1}{\sqrt{2}}(|00\rangle \pm |11\rangle),$$

$$|\Psi^\pm\rangle = \frac{1}{\sqrt{2}}(|01\rangle \pm |10\rangle).$$

Entanglement is a key element in quantum networks as it enables quantum teleportation [13], whose circuit is represented in Fig. 1. This protocol allows nodes to communicate without the transmission of physical particles, i.e., matter qubits, which would be irremediably lost due to attenuation or environment interaction.

For this reason, to teleport an unknown quantum state  $|\varphi\rangle$ , a quantum source distributes through a quantum channel two entangled photons, i.e., flying qubits, characterized by one of the Bell states, e.g.,  $|\Phi^+\rangle$ , to sender and receiver [28]. These flying qubits are converted into communication qubits through a matter-flying transducer [11] and then moved to data qubits leveraging the SWAP instruction [29] to execute operations\*.

This set of operations, known as the Bell State Measurement (BSM), consist of a CNOT gate, followed by an H gate and two quantum measurements. The CNOT gate flips the target qubit  $|\Phi^+\rangle$ , when the control one, e.g.,  $|\varphi\rangle$ , is in the one state  $|1\rangle$ . Otherwise, the target qubit remains unchanged. The H gate is applied on the first qubit and creates a superposition state. Then, the quantum measurements are performed and the results, i.e.,  $c_1$  and  $c_2$ , are transmitted to the receiver through a classical channel. Finally, the receiver retrieves the original state by applying an X or Z gate (or both), according to the correction bits received. It is worth noting that, due to the Bell state measurement, the teleportation destroys the qubits state held by the sender.

### IV. SYSTEM MODEL

This work envisions a quantum network composed of a quantum source, located at  $\mathbf{q} \in \mathbb{R}^2$ , and a group of  $N$  quantum nodes, each one placed in  $\mathbf{u}_n \in \mathbb{R}^2$  with  $n = 1, \dots, N$ .

\*It is worth specifying that both communication and data qubits are physical particles, i.e., matter qubits, but reserved for different purposes.

Symbol	Description	Symbol	Description
$N$	Number of quantum nodes.	$\hat{p}, \bar{p}_m$	Probability that dephasing does not occur at TX/RX.
$M$	Number of quantum node pairs.	$\bar{p}_m$	Dephasing due to different distances from the source.
$\mathbf{q}$	Location of the quantum source.	$P_m$	Overall probability of successfully receive a qubit.
$\mathbf{u}_n$	Location of the quantum node $n$ .	$R_1$	Depolarizing rate.
$\gamma$	Photon distribution plan.	$R_2$	Dephasing rate.
$\bar{\gamma}$	Maximum photon pairs generated by the source.	$\eta$	Attenuation factor of the fiber.
$c$	Propagation speed in the fiber.	$\tau$	Operation time per quantum instruction.
$d_n$	Distance between a node $n$ and the quantum source.	$\rho$	Number of qubits successfully received by the nodes.
$d_m$	Distance between the nodes of couple $m$ .	$\ell$	Sides' length of the square-shaped reference area.
$p_n$	Probability of successfully receiving a photon.	$t_n$	Propagation delay of the quantum channel.
$p_I$	Probability of losing a photon after generation.	$\bar{t}_m$	Propagation delay of the classical channel.
$\bar{p}_m$	Probability of successfully sending classical information.	$\hat{t}, \bar{t}$	Time of operations at sender and receiver.
$\hat{p}$	Probability that qubit depolarization does not occur.	$\Delta_m$	Difference dephasing time.

TABLE I: Main notation adopted in this work.

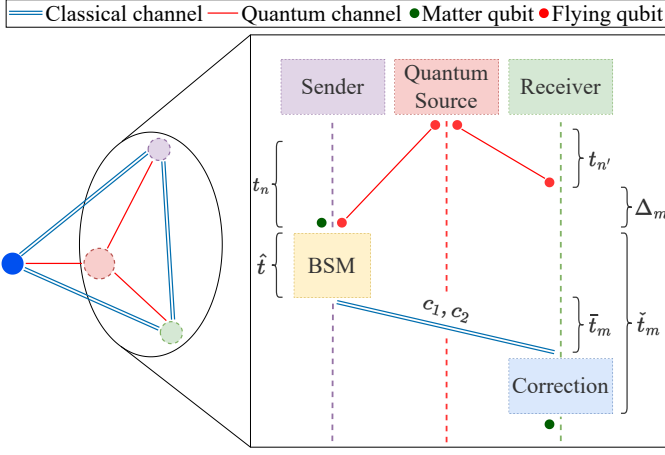


Fig. 2: Sequence diagram of quantum teleportation.

All nodes are connected, via optical fiber, to the quantum source and among themselves [30]. For the sake of notation, each couple of nodes  $(n, n')$ , with  $n \neq n'$ , is denoted by  $m = 1, \dots, M$ , where  $M = \frac{N(N-1)}{2}$ . Each node is equipped with the necessary devices to perform quantum measurements, thus allowing the exchange of quantum states by means of teleportation protocol, whose sequence diagram is depicted in Fig. 2. In this work, it is assumed that (i) the quantum memory is large enough to store the received qubits, for all nodes, and (ii) the quantum source runs for a fixed time window large enough to successfully generate a maximum number of entangled pairs  $\bar{\gamma}$ . For the sake of generality,  $\bar{\gamma}$  is left as a free parameter which however must take into account the success probability related to the generation process, which in turn depends on the specific hardware implementation. Moreover, for each couple of nodes  $m$ , the quantum source allocates  $\gamma_m \in \mathbb{N}$  entangled photon pairs, with  $\gamma = \{\gamma_m\}$ . Clearly, the total number of entangled photon pairs cannot exceed the upper bound  $\bar{\gamma}$ .

#### A. Overall teleportation probability

A wide range of factors may affect the probability of successfully retrieving the quantum state of a transmitted qubit when the teleportation protocol is adopted.

In particular, the distance between the source and the receiver introduces a propagation delay  $t_n = \frac{d_n}{c}$ , where

$d_n = \|\mathbf{q} - \mathbf{u}_n\|$  is the length of the source-node link and  $c$  is the propagation speed in optical fiber.

In addition to the delay, the fiber introduces also attenuation, which can cause the loss of the travelling photon along each path. As a result, the probability of successfully receiving it [22], for each node  $n$ , is:

$$p_n = (1 - p_I)10^{-\frac{\eta d_n}{10}}, \quad (1)$$

where  $p_I$  is the probability of losing the flying qubit immediately after generation due to hardware imperfections, and  $\eta$  is the attenuation factor. Similarly, on the sender side, once the BSM is performed, the information employed for reconstruction is delivered through the classical channel, which introduces a propagation delay  $\bar{t}_m = \frac{\bar{d}_m}{c}$ , where  $\bar{d}_m = \|\mathbf{u}_n - \mathbf{u}_{n'}\|$  is the distance associated to node pair  $m$ . The probability of successfully sending classical information [31], for each couples of nodes  $m$ , can be modelled as:

$$\bar{p}_m = 10^{-\frac{\eta \bar{d}_m}{10}}. \quad (2)$$

Qubits stored in quantum memory are subject to different sources of noise, each one depending on different aspects, such as hardware imperfections and the system-environment interaction. Specifically, errors in the gate operations can lead to bit-flip, phase-flip, or both errors with equal probabilities. All of these have the same probability to occur and can be simulated by the Pauli X, Z, or Y operation, respectively [32]. As a result, gate infidelities can be modelled according to the depolarizing noise and, thus, the probability that qubit depolarization does not occur can be written as follow [22]:

$$\hat{p} = e^{-\tau R_1}, \quad (3)$$

where  $\tau$  is the time spent for the execution of a single operation and  $R_1$  is the depolarizing rate.

Another type of noise is the dephasing one, which arises from the interaction between qubits and their environment, leading to qubit decoherence. The probability of dephasing depends on the amount of time that the qubit stays in memory and can be simulated by stochastically applying the Pauli Z gate [32]. From a sender side, assuming that the qubit encoding the information to be transmitted is generated at the same time as both entangled photons arrive, the probability that qubits do not suffer from dephasing noise [22] is given by:

$$\hat{p} = e^{-\hat{t} R_2}, \quad (4)$$

where  $R_2$  is the dephasing rate and  $\hat{t}$  depends only on the amount of time that the sender requires to perform the Bell state measurement, i.e.  $\hat{t} = 4\tau$ . From a receiver side, instead, the probability can be written as:

$$\check{p}_m = e^{-\check{t}_m R_2}, \quad (5)$$

where  $\check{t}_m$  denotes the amount of time needed to receive the measurement outcome and perform the correction operations, i.e.  $\check{t}_m = \bar{t}_m + 6\tau$ . Besides, since the two communicating nodes can be located at different distances from the source, it is necessary to consider a further time contribution related to the qubit dephasing probability:

$$\dot{p}_m = e^{-\Delta_m R_2}, \quad (6)$$

where  $\Delta_m = |\bar{t}_n - t_{n'}|$ . Note that the above term affects only the node closer to the source. Indeed, when the source is equidistant from both nodes, (6) is zero.

It is important to specify that the time spent for execution of local operations at the sender and the receiver might affect gate infidelity due to depolarizing noise, resulting in higher infidelities. It is also worth mentioning that the depolarizing and dephasing rates can vary depending on the specific quantum hardware used for quantum nodes. Nonetheless, the above modeling can account for these phenomena by considering a larger operation time per instruction  $\tau$ .

Finally, considering (1)-(5), the overall probability of correctly receiving a qubit in the worst case scenario, i.e., in which both X and Z gates are applied at the receiver, is:

$$P_m = p_n p_{n'} \hat{p}^2 \check{p}_m \tilde{p}^7 \bar{p}_m \dot{p}_m, \quad (7)$$

where  $\hat{p}^2$  is the dephasing probability of sender's qubits,  $\tilde{p}^7$  are the probabilities that the depolarization does not occur at both sender and receiver<sup>†</sup>. The exponents of these probabilities correspond to the number of operations performed, as discussed in Section III.

Therefore, after some algebraic manipulation, Eq. (7) can be written as:

$$P_m = a 10^{-\frac{\eta}{10}(d_n + d_{n'} + \bar{d}_m)} e^{-(15\tau + \bar{t}_m + \Delta_m)R_2 - 6\tau R_1}. \quad (8)$$

where  $a = (1 - p_I)^2$ . The above expression, which accounts for all the discussed phenomena, can be used to design and assess a quantum network architecture.

## V. PROBLEM FORMULATION

To enable fair teleportation among quantum nodes, a dedicated strategy for the distribution of entanglement has to be employed. To this aim, it is necessary to optimally derive (i) a photon distribution plan  $\gamma$  and (ii) the position of the quantum source  $\mathbf{q}$ , defined at the beginning of Section IV. Therefore,

<sup>†</sup>In this work, it is assumed the probability of depolarization for one qubit does not depend on the state of others [5]. Therefore, the depolarization related to the CNOT gate must be counted twice, as it affects both control and target qubit.

to derive the optimal entanglement distribution, the following optimization problem is formulated:

$$\max_{\rho, \gamma, \mathbf{q}} \rho \quad \text{s.t.} \quad (9)$$

$$\rho \leq P_m \gamma_m, \quad \forall m = 1, \dots, M, \quad (10)$$

$$\sum_{m=1}^M \gamma_m \leq \bar{\gamma}, \quad (11)$$

$$\gamma \in \mathbb{N}^M \quad (12)$$

Problem (9) aims to fairly maximize the minimum number of qubits  $\rho$  successfully received by each couple of quantum nodes  $m$  through the joint optimization of the scheduling distribution plan  $\gamma$  and the position of the source  $\mathbf{q}$ . In particular, constraint (10) states that  $\rho$  cannot be higher than the average number of photons received by each couple. Equivalently,  $\rho$  guarantees to have a minimum common number of successfully teleported qubits in the quantum network. Moreover, constraint (11) limits the number of entangled photon pairs generated by a maximum value  $\bar{\gamma}$ . Finally, (12) imposes that the number of assigned photon couples is always a positive integer.

## VI. PROPOSED SOLUTION

As immediate results from its formulation, (9) is a non-convex programming problem, which is challenging to solve. Specifically, constraint (10) couples the scheduling plan  $\gamma$  with the source position  $\mathbf{q}$ , which is encompassed in the distance  $d_n$  within probability  $P_m$ . To cope with these issues, problem (9) is split into two sub-problems which are separately solved to derive an optimal solution.

### A. Sub-problem 1: Photon pair distribution

Given the optimal quantum source location,  $\rho$  is employed to fairly maximize the photon distribution with respect to the scheduling plan. Therefore, the first sub-problem reads

$$\max_{\rho, \gamma} \rho \quad \text{s.t.} \quad (10), (11), (12). \quad (13)$$

which is non-convex, due to constraint (12). Nonetheless, (13) can be relaxed by neglecting such a constraint, thus becoming a convex optimization problem whose solution can be then rounded with a floor operation. Hence, a generic solver can be employed at the cost of computational complexity in the order of  $\mathcal{O}((M+1)^{3.5})$ . To reduce such complexity, the KKT conditions [26] can be applied to derive a closed-form solution.

**Theorem 1.** *The optimal photon distribution plan, for each couple of nodes  $m$ , and the maximum number of qubits per node are*

$$\gamma_m = \bar{\gamma} \left( P_m \sum_{m'=1}^M \frac{1}{P_{m'}} \right)^{-1}, \quad \rho = \bar{\gamma} \left( \sum_{m=1}^M \frac{1}{P_m} \right)^{-1}, \quad (14)$$

which only depend on the position of the quantum source embedded in the probabilities  $P_m$ .

*Proof.* The Langrangian function corresponding to the relaxed problem (13) is

$$\mathcal{L} = \rho - \sum_{m=1}^M \lambda_m (\rho - P_m \gamma_m) - \mu \left( \sum_{m=1}^M \gamma_m - \bar{\gamma} \right),$$

where  $\lambda_m \geq 0$  and  $\mu \geq 0$  are the multipliers related to the constraints (10) and (11), respectively. Therefore, the KKT conditions read

$$\frac{\partial \mathcal{L}}{\partial \rho} = 1 - \sum_{m=1}^M \lambda_m = 0, \quad (15)$$

$$\frac{\partial \mathcal{L}}{\partial \gamma_m} = \lambda_m P_m - \mu = 0, \quad \forall m, \quad (16)$$

$$\lambda_m (\rho - P_m \gamma_m) = 0, \quad \forall m, \quad (17)$$

$$\mu \left( \sum_{m=1}^M \gamma_m - \bar{\gamma} \right) = 0. \quad (18)$$

The first two equations are sufficient to demonstrate that the multipliers are strictly positive:

$$\frac{\mu}{P_m} = \lambda_m \Rightarrow \mu \sum_{m=1}^M \frac{1}{P_m} = \sum_{m=1}^M \lambda_m \Rightarrow \mu = \left( \sum_{m=1}^M \frac{1}{P_m} \right)^{-1},$$

where the third equality is due to (15). Therefore, the last two conditions leads to

$$\bar{\gamma} = \sum_{m=1}^M \gamma_m, \quad (19)$$

$$\begin{aligned} \rho - P_m \gamma_m = 0 &\Rightarrow \rho \sum_{m=1}^M \frac{1}{P_m} = \sum_{m=1}^M \gamma_m = \bar{\gamma} \Rightarrow \\ \rho &= \bar{\gamma} \left( \sum_{m=1}^M \frac{1}{P_m} \right)^{-1} \Rightarrow \gamma_m = \frac{\rho}{P_m}. \end{aligned} \quad (20)$$

□

**Corollary 1.** *The entanglement distribution plan becomes uniform, i.e.,  $\gamma_m = 2\bar{\gamma}/(N(N-1)) \forall m$ , when the probabilities  $P_m \rightarrow P \in [0, 1] \forall m$ , leading to the maximum number of qubits per link  $\rho = \bar{\gamma}P$ . This phenomenon takes place when the impact of the distances among the nodes is negligible. It occurs in two cases: (i) the inter-node distances are similar, which is topologically challenging with a significant number of quantum nodes, and (ii) the area in which the nodes are deployed is small enough, i.e., in the order of a few kilometers.*

**Corollary 2.** *As a result of the above theorem,  $\rho$  can now be defined as the average number of qubits successfully received by each couple of nodes  $m$ .*

The computational complexity of the procedure to calculate the optimal solution is  $\mathcal{O}(2M+1) = \mathcal{O}(M)$ , since the single complexities to compute  $\rho$  and  $\gamma$  are both linear with respect to the number of node pairs.

## B. Sub-problem 2: Quantum source position

The second sub-problem aims to derive the optimal source location  $\mathbf{q}$ , given a fixed scheduling plan  $\gamma$  and the definition of  $\rho$  obtained in (20). Hence, (9) can be written as:

$$\max_{\mathbf{q}} \rho \quad \text{s.t.} \quad (10). \quad (21)$$

However, problem (21) is non-convex due to the presence of  $\mathbf{q}$  in the exponent of  $P_m$ . To tackle this issue, let equivalently rearrange (8) as

$$P_m = \alpha_m 10^{-\frac{\eta}{10}(d_n + d_{n'}) - \beta|d_n - d_{n'}|}, \quad (22)$$

with

$$\alpha_m = a 10^{-\frac{\eta}{10} \bar{d}_m} e^{-(15\tau + \bar{t}_m)R_2 - 6\tau R_1}, \quad (23)$$

and  $\beta = \frac{R_2}{\ln(10)c}$ . Then, recalling the definition of  $\rho$  and  $\gamma$  derived from Theorem 1, substituting (14) in (21) leads to

$$\max_{\mathbf{q}} \left( \sum_{m=1}^M \frac{1}{P_m} \right)^{-1} = \min_{\mathbf{q}} \sum_{m=1}^M \alpha_m^{-1} 10^{\frac{\eta}{10}(d_n + d_{n'}) + \beta|d_n - d_{n'}|}, \quad (24)$$

which is still intractable due to the presence of the module term that depends on  $\mathbf{q}$  through the difference of the nodes' distances. To cope with the non-convexity of the above, a vector composed by  $M$  slack variables  $\mathbf{r} = [r_1, \dots, r_M]^T$  is introduced as well as the following constraints

$$\|\mathbf{q} - \mathbf{u}_n\| - \|\mathbf{q} - \mathbf{u}_{n'}\| \leq r_m, \quad \forall m = 1, \dots, M, \quad (25)$$

which can be squared on both sides and manipulated as

$$\begin{aligned} \|\mathbf{q} - \mathbf{u}_n\|^2 + \|\mathbf{q} - \mathbf{u}_{n'}\|^2 - 2\|\mathbf{q} - \mathbf{u}_n\|\|\mathbf{q} - \mathbf{u}_{n'}\| \\ = 2\left(\|\mathbf{q} - \mathbf{u}_n\|^2 + \|\mathbf{q} - \mathbf{u}_{n'}\|^2\right) \\ - (\|\mathbf{q} - \mathbf{u}_n\| + \|\mathbf{q} - \mathbf{u}_{n'}\|)^2 \leq r_m^2. \end{aligned} \quad (26)$$

Then, the SCA technique [33] is applied. Indeed, reminding that the first-order Taylor expansion is a global underestimator for convex functions, (26) can be approximated as

$$\begin{aligned} 2\left(\|\mathbf{q} - \mathbf{u}_n\|^2 + \|\mathbf{q} - \mathbf{u}_{n'}\|^2\right) - (\|\bar{\mathbf{q}} - \mathbf{u}_n\| + \|\bar{\mathbf{q}} - \mathbf{u}_{n'}\|)^2 \\ - 2\left(\frac{\bar{\mathbf{q}} - \mathbf{u}_n}{\|\bar{\mathbf{q}} - \mathbf{u}_n\|} + \frac{\bar{\mathbf{q}} - \mathbf{u}_{n'}}{\|\bar{\mathbf{q}} - \mathbf{u}_{n'}\|}\right)^T (\|\bar{\mathbf{q}} - \mathbf{u}_n\| + \|\bar{\mathbf{q}} - \mathbf{u}_{n'}\|) \\ \times (\mathbf{q} - \bar{\mathbf{q}}) \leq \bar{r}_m^2 + 2\bar{r}_m(r_m - \bar{r}_m) \end{aligned} \quad (27)$$

where  $\bar{\mathbf{q}}$  and  $\bar{\mathbf{r}} = [\bar{r}_1, \dots, \bar{r}_M]^T$  are the local point of the expansion. Finally, given the above convex set of constraints, problem (24) can be reformulated as

$$\min_{\mathbf{q}, \mathbf{r}} \xi \triangleq \sum_{m=1}^M \alpha_m^{-1} 10^{\frac{\eta}{10}(d_n + d_{n'}) + \beta r_m} \quad \text{s.t.} \quad (27), \quad (28)$$

which can be iteratively solved until convergence to a prescribed tolerance  $\epsilon$  is achieved [33], since its convexity is proved in the following Theorem.

**Theorem 2.** *Problem (28) is convex and can be solved with a generic optimization tool, such as CVX.*

*Proof.* The convexity of the objective function is guaranteed as (i) the euclidean norm is convex, (ii) the sum of convex functions is convex, and (iii) the composition  $g(f(x))$  of a convex



---

**Algorithm 1** Proposed algorithm
 

---

- 1: Initialize the quantum node positions  $\mathbf{u}_n$ ;
  - 2: Compute the probabilities  $P_m$  derived in (8);
  - 3: Randomly initialize local points  $\bar{\mathbf{q}}$  and  $\bar{\mathbf{r}}$ ;
  - 4: **repeat**
  - 5:   Solve (28) to obtain the optimal  $\mathbf{q}$  and  $\mathbf{r}$ ;
  - 6:    $\bar{\mathbf{q}} \leftarrow \mathbf{q}$ ;
  - 7:    $\bar{\mathbf{r}} \leftarrow \mathbf{r}$ ;
  - 8: **until** convergence is achieved
  - 9: According to Theorem 1, compute the photon distribution plan  $\gamma$  and the maximum number of qubits per quantum node  $\rho$ ;
- 

non-decreasing function  $g(y)$  and a convex function  $f(x)$  is convex as well. Moreover, constraints (27) are quadratic in the source position and linear in the slack variables, and hence convex by definition.  $\square$

**Remark 1.** *It is worth noting that, even if the source position has a non-linear effect over the objective function in (28), the optimal solution is intuitively the centroid computed over the quantum nodes' positions, when these are uniformly deployed over the area. Indeed, it minimizes all  $d_n$  at the same time.*

The computational complexity of the optimization procedure, due to the summation of the inverse probabilities in (28), is  $\mathcal{O}(K(M + (M + 2)^{3.5})) = \mathcal{O}(KM^{3.5})$  with  $K$  being the number of iterations of the SCA procedure.

### C. Overall algorithm and complexity

The overall optimization procedure, summarized in Algorithm 1, derives the optimal location of the quantum source by leveraging the optimal closed-form expression of the maximum number of qubits per node. The total computational complexity, obtained as the sum of the single complexities, is  $\mathcal{O}(KM^{3.5}) + \mathcal{O}(M) = \mathcal{O}(KM^{3.5})$ .

## VII. PERFORMANCE EVALUATION AND RESULTS

A simulation campaign is carried out to analyze and validate the findings of this work.

The first part investigates the impact of different parameter settings, such as (i) dephasing rate  $R_2$ , (ii) initial probability of losing a photon once it enters a channel  $p_I$ , (iii) the attenuation factor  $\eta$ , and (iv) inter-node distance  $\bar{d}_m$ , on the overall probability derived in (8).

In the second part, the results obtained from the proposed optimization algorithm are discussed and compared with a baseline approach. The latter exploits the optimal solution derived in sub-problem 1 for what concerns the scheduling plan, while for the position of the quantum source it adopts the centroid computed over the quantum nodes' locations. The analysis focuses on the impact that system conditions, which are made varying, have on the network performance.

According to [22] and [24], the considered configuration parameters in all simulations, unless otherwise specified, are  $p_I = 0.1$ ,  $\eta = 0.1$  dB/km,  $R_1 = 10$  kHz,  $R_2 = 0.1$  MHz,  $\epsilon = 10^{-6}$ ,  $\tau = 10$  ns,  $\bar{\gamma} = 1.2 \cdot 10^9$ , and  $c = 2 \cdot 10^5$

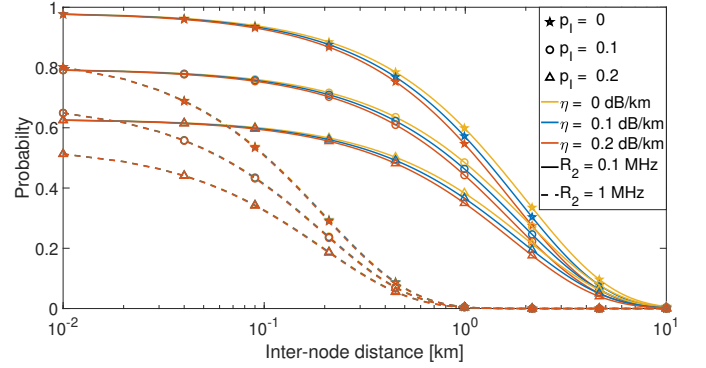


Fig. 3: Overall probability of correctly receiving a qubit.

km/s. The quantum nodes are deployed in square-shaped areas with all sides having a length of  $\ell$ . In all the simulation two different methodologies are employed to generate the nodes' coordinates: the first consists in sampling the positions of all nodes from circumference, i.e.,  $U_1 \sim \mathcal{C}(0, \ell)$ ; the second one generates the locations according to a uniform distribution  $U_2 \sim \mathcal{U}(0, \ell)$ ; the third samples from a beta distribution  $U_3 \sim \text{Beta}(0.5, 0.5)$ ; the fourth generates the positions following a triangular distribution  $U_4 \sim \mathcal{T}(0, 0.5, 1)$ ; the fifth  $U_5$  distributes half of the nodes from  $U_2$  and the second one from a scaled version of it, i.e.,  $\mathcal{U}(0, \ell/3)$ .

### A. Analysis on the overall teleportation probability

In the first scenario, a quantum network composed of  $N = 2$  quantum nodes, i.e.,  $M = 1$ , is considered. Specifically, the nodes are aligned along an axis and the quantum source is placed exactly in the middle. Thus, the inter-node distance  $\bar{d}_1$  is varied from 0 km to 2 km. This initial analysis highlights the significant challenges in transmitting quantum information over long distances due to the loss and noise in the transmission channel.

The results, as shown in Fig. 3, confirm that the probability of correctly receiving a qubit exponentially decreases as the inter-node distance grows. This effect is highly influenced by the dephasing rate, which affects the decoherence probability of qubits, especially at the receiver node. Notably, when the dephasing rate is set to 1 MHz, the probability drops close to zero once the inter-node distance reaches 1 km. For  $R_2 = 0.1$  MHz, instead, it almost zeros out around 10 km. Another parameter that significantly affects the overall probability is  $p_I$ , which, regardless of other parameters, causes the curves in Fig. 3 to start at a higher value and decline more gradually to zero. Therefore, the dephasing rate and the generation probability, which are associated with the technology on which the system is based on, represent fundamental aspects to potentially expand the network area and hence to assess the feasibility of quantum teleportation.

### B. Impact of the topology

In this simulation, a quantum network consisting of  $N = 10$  nodes, distributed in an area characterized by  $\ell = 5$  km, is

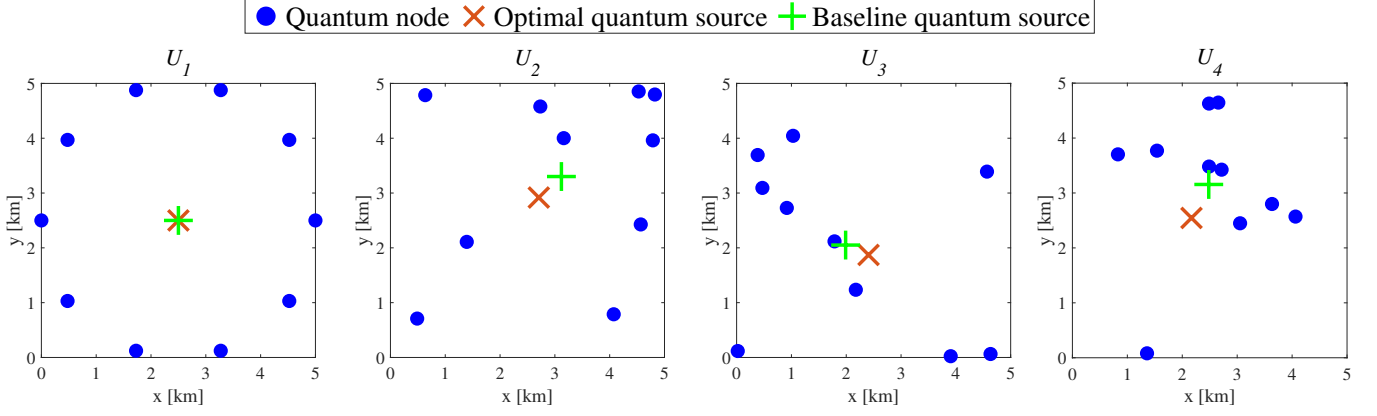


Fig. 4: Optimal and Baseline quantum source position with  $N = 10$  nodes in different topologies.

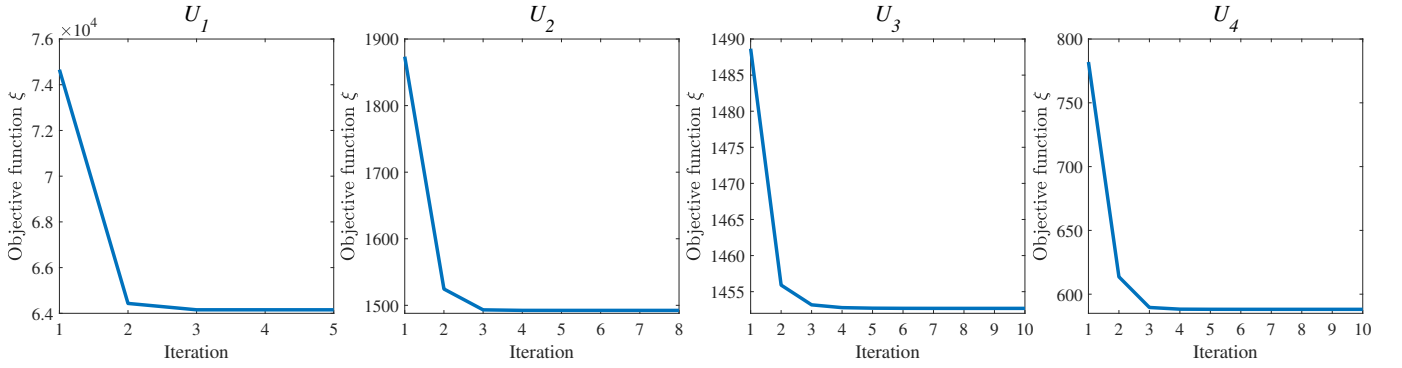


Fig. 5: Convergence curves of the proposed algorithm.

considered. Four different topologies, generated according to  $U_1, U_2, U_3$ , and  $U_4$ , are examined.

Fig. 4 illustrates the comparison between the baseline and the proposed approach for the optimal positioning of the quantum source. In the first considered topology, all nodes are equidistant from the same point, i.e., the center of the circumference, which is the optimal position to deploy the quantum source, thus proving Remark 1. Indeed, both algorithms achieve the same solution in terms of source location and minimum number of successfully received qubits  $\rho = 3.8 \cdot 10^5$ . However, in the case of a random distribution, the optimal position of the source is not the centroid. As a matter of fact, the optimal source location cannot be simply derived by averaging the nodes positions, which would lead to worse performance. Indeed, considering the last three topologies, the baseline approach achieves a minimum number of transmitted qubit  $\rho$  of  $2.6 \cdot 10^6$ ,  $1.6 \cdot 10^6$ , and  $2.7 \cdot 10^6$ , respectively, whereas the proposed approach reaches a remarkable  $3.3 \cdot 10^6$ ,  $2 \cdot 10^6$ , and  $3.7 \cdot 10^6$ , which corresponds to a minimum increase of 25%. Finally, Fig. 5 shows the convergence of the proposed algorithm in both topologies in terms of the objective function  $\xi$  defined in Eq. (28), which represents a local approximation of  $\rho$  in the iterative optimization process. Clearly, the number of iterations required to converge in the first case is smaller with respect to the other configurations, due to the regular shape of the network graph.

### C. Impact of the system parameters

To assess the impact of the inter-node distance on the entanglement distribution,  $N = 20$  quantum nodes are sampled from  $U_5$  and deployed within various areas characterized by  $\ell \in [0, 20]$  km.

In particular, Fig. 6 shows the quantum source location for both the considered algorithm, when  $\ell = \{1, 5, 10, 20\}$ . As can be seen, the source position provided by the baseline approach remains the same, i.e., the centroid, except for the scale. On the contrary, the proposed solution changes with  $\ell$ , thus demonstrating to be able to capture the non-linearity of the probability expression derived in Section IV. It is worth noting that, in case of  $\ell = 1$  km, the area is small enough to adopt the baseline as quasi-optimal solution. Indeed, the impact of the inter-node distances is negligible in small areas, as predicted by Corollary 1. To further corroborate the above findings and to give more insights about the performance gain provided by the optimal algorithm, Fig. 7 depicts the trend of  $\rho$  as a function of  $\ell \in [0, 20]$ . As a matter of fact, for a limited area the solutions are comparable but as  $\ell$  increases, a major gap in terms of successfully received qubits arises. This demonstrates the crucial importance of the proposed optimal design in case of quantum networks deployed, especially, in wide areas. Specifically for  $R_2 = 0.1$  MHz and  $\ell = 20$  km, the optimal algorithm allows the transmission of 124 qubits for  $\eta = 0.1$  and 52 qubits for  $\eta = 0.2$ , while the baseline approach just 6 and 2 qubits. As a consequence, the proposed



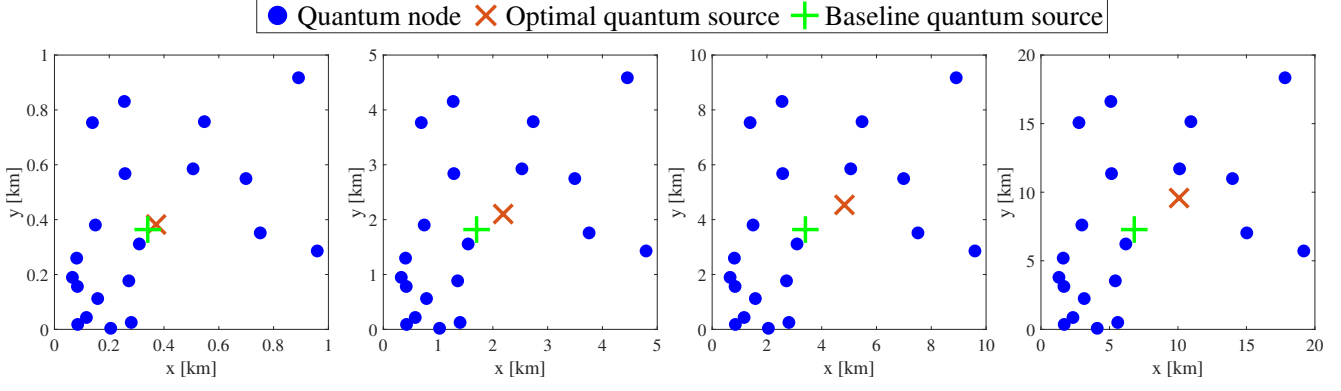


Fig. 6: Comparison between optimal and baseline approaches with fixed topology of  $N = 20$  nodes deployed within areas of different scale.

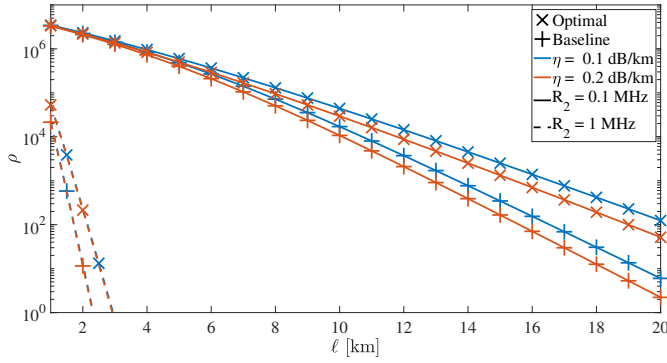


Fig. 7: Number of correctly received qubits  $\rho$  as a function of  $\ell$  for different system parameters.

algorithm provides, in terms of received qubits,  $\sim 20$  and  $\sim 25$  times better solutions, respectively. In case of higher dephasing rate  $R_2 = 1$  MHz, the resulting loss constrains the maximum possible area, thus producing no difference between the two algorithms, which again confirms Corollary 1.

#### D. Analysis on network scalability

In this last analysis, the impact of the number of nodes in a quantum network having  $\ell = 10$  km is investigated. In this regard, a Monte Carlo simulation is carried out by generating the nodes' positions according to both  $U_2$  and  $U_5$ , for a total of  $10^3$  samples. This procedure is iterated by making the number of nodes vary, i.e.,  $N = \{10, 20, 30, 40, 50\}$ .

Figure 8 and Figure 9 illustrate the relationship between  $\rho$  and the number of nodes for  $U_2$  and  $U_5$ , respectively. As expected, in both cases, the proposed and the baseline approaches exhibit a decreasing trend as the number of nodes increases. This is due to the reduction in the number of entangled pairs available for each pair of nodes as the network size grows. Notably, the proposed algorithm performs better than the baseline approach, in terms of number of transmitted qubits with a much smaller variance, in both cases. Nonetheless, this difference becomes more evident when the nodes are generated according to  $U_5$ . Vice versa, as already stated in Remark 1 and proved in Section VII-B, when  $U_2$  is chosen, i.e., the

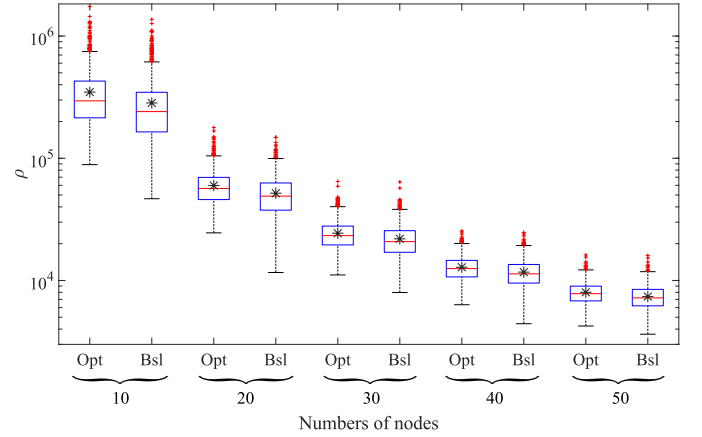


Fig. 8: Comparison between proposed (Opt) and baseline (Bsl) approaches with respect to  $\rho$  as a function of quantum nodes  $N$  with  $U_2$ . The black stars represent the mean value.

uniform distribution, the optimal source position becomes the centroid of the network. Therefore, the proposed and baseline approaches perform similarly, even if the former still provides better results. Specifically, when considering  $U_2$  with  $N = 50$ , the proposed algorithm and the baseline approach achieve a mean value of  $\rho = 8 \cdot 10^3$  and  $\rho = 7 \cdot 10^3$ , whereas for  $U_5$ , they attain a  $\rho = 9 \cdot 10^3$  and  $\rho = 3 \cdot 10^3$ , respectively.

## VIII. CONCLUSIONS

This work investigates the achievable performance of a quantum network through the mathematical modeling of the probability that a qubit successfully reaches the receiver node. Differently from other contributions, the derived expression considers multiple sources of impairment affecting the teleportation protocol. Starting from this model, a MINLP problem, aiming at fairly maximizing the number of qubits received by nodes, is formulated. Therefore, the optimal entanglement distribution and quantum source position are compared with a baseline approach. The latter considers the same methodology to derive the optimal photon distribution plan but employs the centroid, computed over the nodes' positions, as quantum source location. The obtained results show the

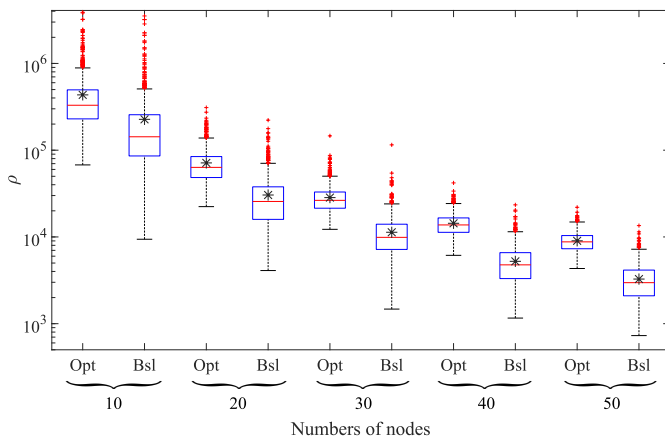


Fig. 9: Comparison between proposed (Opt) and baseline (Bsl) approaches with respect to  $\rho$  as a function of quantum nodes  $N$  with  $U_5$ . The black stars represent the mean value.

significant performance gap between the two algorithms, in terms of number of qubits exchanged per node pair. Overall, the conducted study highlights the significant challenges in transmitting quantum information over long distances due to the loss and noise in the transmission channel. At the same time, the derived theoretical findings become crucial for designing and optimizing quantum communication networks, which have immense potential to revolutionize communication and computation. Future research efforts will focus on investigating the teleportation of high-dimensional quantum states, comparing the performance of different quantum source models, and precisely computing and optimizing fidelity in the presence of multiple repeaters.

## REFERENCES

- [1] L. Gyongyosi and S. Imre, "A survey on quantum computing technology," *Comput. Sci. Rev.*, vol. 31, pp. 51–71, 2019.
- [2] A. W. Harrow and A. Montanaro, "Quantum computational supremacy," *Nature*, vol. 549, no. 7671, pp. 203–209, 2017.
- [3] G. T. Byrd and Y. Ding, "Quantum computing: Progress and innovation," *Computer*, vol. 56, no. 1, pp. 20–29, 2023.
- [4] A. S. Cacciapuoti, M. Caleffi, F. Tafuri, F. S. Cataliotti, S. Gherardini, and G. Bianchi, "Quantum internet: Networking challenges in distributed quantum computing," *IEEE Network*, vol. 34, no. 1, pp. 137–143, 2020.
- [5] M. A. Nielsen and I. L. Chuang, *Quantum Computation and Quantum Information: 10th Anniversary Edition*. Cambridge University Press, 2010.
- [6] J. Preskill, "Quantum computing in the nisq era and beyond," *Quantum*, vol. 2, p. 79, 2018.
- [7] H. J. Kimble, "The quantum internet," *Nature*, vol. 453, no. 7198, pp. 1023–1030, 2008.
- [8] M. Caleffi, A. S. Cacciapuoti, and G. Bianchi, "Quantum internet: From communication to distributed computing!" in *Proceedings of the 5th ACM International Conference on Nanoscale Computing and Communication*, ser. NANOCOM '18. New York, NY, USA: Association for Computing Machinery, 2018.
- [9] S. Wehner, D. Elkouss, and R. Hanson, "Quantum internet: A vision for the road ahead," *Science*, vol. 362, 2018.
- [10] F. Vista, V. Musa, G. Piro, L. A. Grieco, and G. Boggia, "Network intelligence with quantum computing in 6g and b6g: Design principles and future directions," in *2021 IEEE Globecom Workshops (GC Wkshps)*. IEEE, 2021, pp. 1–6.
- [11] D. Cuomo, M. Caleffi, and A. S. Cacciapuoti, "Towards a distributed quantum computing ecosystem," *IET Quantum Communication*, 2020.
- [12] R. Horodecki, P. Horodecki, M. Horodecki, and K. Horodecki, "Quantum entanglement," *Reviews of modern physics*, vol. 81, no. 2, p. 865, 2009.
- [13] C. H. Bennett, G. Brassard, C. Crépeau, R. Jozsa, A. Peres, and W. K. Wootters, "Teleporting an unknown quantum state via dual classical and einstein-podolsky-rosen channels," *Phys. Rev. Lett.*, vol. 70, pp. 1895–1899, Mar 1993.
- [14] J. Illiano, M. Caleffi, A. Manzalini, and A. S. Cacciapuoti, "Quantum internet protocol stack: A comprehensive survey," *Computer Networks*, p. 109092, 2022.
- [15] W. Kozłowski, A. Dahlberg, and S. Wehner, "Designing a quantum network protocol," in *Proceedings of the 16th International Conference on Emerging Networking EXperiments and Technologies*, ser. CoNEXT '20. New York, NY, USA: Association for Computing Machinery, 2020, p. 1–16.
- [16] K. Chakraborty, D. Elkouss, B. Rijsman, and S. Wehner, "Entanglement distribution in a quantum network: A multicommunity flow-based approach," *IEEE Transactions on Quantum Engineering*, vol. 1, pp. 1–21, 2020.
- [17] C. Li, T. Li, Y.-X. Liu, and P. Cappellaro, "Effective routing design for remote entanglement generation on quantum networks," *npj Quantum Information*, vol. 7, no. 1, p. 10, 2021.
- [18] J. Li, M. Wang, K. Xue, R. Li, N. Yu, Q. Sun, and J. Lu, "Fidelity-guaranteed entanglement routing in quantum networks," *IEEE Transactions on Communications*, vol. 70, no. 10, pp. 6748–6763, 2022.
- [19] Y. Zhao, G. Zhao, and C. Qiao, "E2e fidelity aware routing and purification for throughput maximization in quantum networks," in *IEEE INFOCOM 2022 - IEEE Conference on Computer Communications*, 2022, pp. 480–489.
- [20] W. Dai, T. Peng, and M. Z. Win, "Quantum queuing delay," *IEEE Journal on Selected Areas in Communications*, vol. 38, no. 3, pp. 605–618, 2020.
- [21] —, "Optimal remote entanglement distribution," *IEEE Journal on Selected Areas in Communications*, vol. 38, no. 3, pp. 540–556, 2020.
- [22] C. Cicconetti, M. Conti, and A. Passarella, "Request scheduling in quantum networks," *IEEE Transactions on Quantum Engineering*, vol. 2, pp. 2–17, 2021.
- [23] L. Chen, K. Xue, J. Li, N. Yu, R. Li, J. Liu, Q. Sun, and J. Lu, "A heuristic remote entanglement distribution algorithm on memory-limited quantum paths," *IEEE Transactions on Communications*, vol. 70, no. 11, pp. 7491–7504, 2022.
- [24] M. Chehimi and W. Saad, "Entanglement rate optimization in heterogeneous quantum communication networks," in *2021 17th International Symposium on Wireless Communication Systems (ISWCS)*. IEEE, 2021, pp. 1–6.
- [25] C. Qiao, Y. Zhao, G. Zhao, and H. Xu, "Quantum data networking for distributed quantum computing: Opportunities and challenges," in *IEEE INFOCOM 2022 - IEEE Conference on Computer Communications Workshops (INFOCOM WKSHPS)*, 2022, pp. 1–6.
- [26] S. P. Boyd and L. Vandenberghe, *Convex optimization*. Cambridge university press, 2004.
- [27] J.-W. Pan, C. Simon, Č. Brukner, and A. Zeilinger, "Entanglement purification for quantum communication," *Nature*, vol. 410, no. 6832, pp. 1067–1070, 2001.
- [28] A. S. Cacciapuoti, M. Caleffi, R. Van Meter, and L. Hanzo, "When entanglement meets classical communications: Quantum teleportation for the quantum internet," *IEEE Transactions on Communications*, vol. 68, no. 6, pp. 3808–3833, 2020.
- [29] J. Illiano, A. S. Cacciapuoti, A. Manzalini, and M. Caleffi, "The impact of the quantum data plane overhead on the throughput," in *Proceedings of the Eight Annual ACM International Conference on Nanoscale Computing and Communication*, ser. NANOCOM '21. New York, NY, USA: Association for Computing Machinery, 2021.
- [30] L. Gyongyosi, S. Imre, and H. V. Nguyen, "A survey on quantum channel capacities," *IEEE Communications Surveys & Tutorials*, vol. 20, no. 2, pp. 1149–1205, 2018.
- [31] G. Vardoyan, S. Guha, P. Nain, and D. Towsley, "On the stochastic analysis of a quantum entanglement distribution switch," *IEEE Transactions on Quantum Engineering*, vol. 2, pp. 1–16, 2021.
- [32] Z. Babar, D. Chandra, H. V. Nguyen, P. Botsinis, D. Alanis, S. X. Ng, and L. Hanzo, "Duality of quantum and classical error correction codes: Design principles and examples," *IEEE Communications Surveys & Tutorials*, vol. 21, no. 1, pp. 970–1010, 2019.
- [33] G. Scutari and Y. Sun, *Parallel and Distributed Successive Convex Approximation Methods for Big-Data Optimization*. Springer International Publishing, 2018.



**Giovanni Iacovelli** received the Ph.D. in electrical and information engineering from Politecnico di Bari, Bari, Italy, in December 2022. His research interests include Internet of Drones, Machine Learning, Optimization and Telecommunications. Currently, he is a Research Fellow at the Department of Electrical and Information Engineering, Politecnico di Bari.



**Francesco Vista** received the Dr. Eng. degree (with honors) in Computer Science Engineering from Politecnico di Bari, Bari, Italy in October 2020. His research interests include Quantum Internet, Quantum communication, and Quantum Optimization. Since 2020, he has been a Ph.D. student at the Department of Electrical and Information Engineering at Politecnico di Bari.



**Nicola Cordeschi** received the five-year Laurea degree (summa cum laude) in communication engineering and the PhD degree in information and communication engineering from the Sapienza University of Rome in 2004 and 2008, respectively. He was Fellow Researcher with the DIET Dept., Sapienza University of Rome for ten years, and Assistant Professor from 2009 to 2016. Then he worked with DIMES Department, University of Calabria. From 2020 to 2022 he was with 6G Innovation Centre, University of Surrey, UK. Since 2022 he has been

Assistant Professor in Telecommunication with the Politecnico di Bari, Italy. He is a recipient of two Best Paper Awards and has authored or coauthored over 80 papers, many of which published in premier network journals and conferences including IEEE TMC, TVT, TCOM, IEEE/ACM TON, and more. His research interests include adaptive wireless communications, internet of things, cognitive radio access, medium access control, random access, multi-antenna systems, energy-efficiency, resource management in vehicular communications, grid/cloud computing, distributed computing, cross-layer optimization, mathematical optimization, game theory.



**L. Alfredo Grieco** is a full professor in telecommunications at Politecnico di Bari. Formerly he has been visiting researcher with INRIA (Sophia Antipolis, France) in 2009 and with LAAS-CNRS (Toulouse, France) in 2013, working on Internet measurements and M2M systems, respectively. He has authored more than 100 scientific papers published in international journals and conferences. He serves as editor of the IEEE Transactions on Vehicular Technology (for which he has been awarded as top associate editor in 2012) and as executive

editor of the Transactions on Emerging Telecommunications Technologies (Wiley). Within the IETF and IRTF, he is actively contributing to the definition of new standard protocols for industrial IoT applications and new standard architectures for ICN-IoT systems. His main research interests include TCP congestion control, quality of service in wireless networks, IoT, and Future Internet.